

Adversarial Robustness of AI-Generated Image Detectors in the Real World

Sina Mavali*, Jonas Ricker†, David Pape*, Asja Fischer†, Lea Schönherr*

*CISPA Helmholtz Center for Information Security

†Ruhr University Bochum

Abstract—The rapid advancement of generative artificial intelligence (GenAI) capabilities is accompanied by a concerning rise in its misuse. In particular the generation of credible misinformation in the form of images poses a significant threat to the public trust in democratic processes. Consequently, there is an urgent need to develop tools to reliably distinguish between authentic and AI-generated content. The majority of detection methods are based on neural networks that are trained to recognize forensic artifacts. In this work, we demonstrate that current state-of-the-art classifiers are vulnerable to adversarial examples under real-world conditions. Through extensive experiments, comprising four detection methods and five attack algorithms, we show that an attacker can dramatically decrease classification performance, without internal knowledge of the detector’s architecture. Notably, most attacks remain effective even when images are degraded during the upload to, e.g., social media platforms. In a case study, we demonstrate that these robustness challenges are also found in commercial tools by conducting black-box attacks on HIVE, a proprietary online GenAI media detector. In addition, we evaluate the robustness of using generated features of a robust pre-trained model and showed that this increases the robustness, while not reaching the performance on benign inputs. These results, along with the increasing potential of GenAI to erode public trust, underscore the need for more research and new perspectives on methods to prevent its misuse.¹

Index Terms—AI-generated image detection, adversarial robustness

1. Introduction

The creation of synthetic visual media is no longer a compelling vision, but has become part of everyday life and a vital business. Within seconds, images with any desired content can be created using state-of-the-art generative models [1]–[3] using a text prompt in most Large Language Model (LLM) chat interfaces. Recently, the quality of synthetic images has reached a level at which humans cannot distinguish them from real media [4]. Thus, although GenAI can support us in productive and creative tasks, the potential for misuse poses unprecedented challenges to our

digital society. As reported by Europol and the FBI, GenAI is increasingly being used for criminal activities, including identity theft and evidence manipulation [5], [6]. Recently, it has also been shown that GenAI is used to create fake identities on social media platforms [7]. In addition, AI-generated disinformation can discredit individuals, manipulate public opinion, and erode trust in democratic processes. The most notable misuse of GenAI so far has been observed in the course of the 2024 US presidential election. Several times, AI-generated images were used to influence voters [8], [9], like the case of Donald Trump sharing synthetic images of Taylor Swift fans, falsely depicted as endorsing him [10]. Often, these images are widely shared on various social media platforms before being removed. These incidents underscore how easily AI-generated images can affect global political landscapes and damage public trust.

Fortunately, legislators and the industry are reacting to this growing threat. Both the US Government [11] and the European Union [12] passed regulations requiring the labeling of synthetic content. However, the task of *reliably*, *robustly*, and *practically* revealing the origin of digital images is far from solved.

Proactive methods such as watermarking [13], [14] and cryptographically signed metadata in image files [15] are not easy to deploy: (i) These methods require that all parties involved agree on the same standard and cooperate, (ii) adversaries could use custom generative models, or (iii) simply remove the metadata or watermark before distributing harmful images [16], [17].

An approach that does not require the cooperation of model providers is to detect synthetic images passively based on forensic artifacts. With enough examples of real and generated images, a model is trained to distinguish generated and real images with high accuracy [18]–[21]. Here, detectors based on standard convolutional neural network (CNN) architectures [18], [19] were considered to be the most effective for a long time. Recently, the approach of using features from a pre-trained foundation model such as CLIP [22] is gaining traction. Detectors that are built on these features have been shown to generalize better to images from unseen generative models [20], [21].

Despite these advances, the adversarial robustness of such detectors—especially in real-world scenarios—remains underexplored. Existing work typically evaluates white-box settings or relies on simple perturbation-based attacks, with-

1. <https://github.com/smavali/AIGI-Break>

out accounting for real-world post-processing or black-box deployment settings [23], [24].

However, detection systems deployed in closed systems, such as those on social media platforms or utilized by journalistic organizations and government entities, are generally not disclosed, nor are their preprocessing steps. In addition, the rapidly growing field of GenAI makes it hard to investigate the robustness of detection models against AI-generated images (AIGIs) generated with future models and the transferability of strong attacks.

This work bridges the gap between modern AIGI detection and adversarial robustness under realistic, deployment-oriented constraints. Our evaluation encompasses state-of-the-art detectors, including four research-based models that utilize CLIP-based features and diffusion model training, alongside a prominent commercial AIGI detector.

To assess robustness in practical settings, we simulate black-box scenarios where the internal workings of the detection system are unknown. This mirrors conditions relevant for detectors deployed on social media or by content moderation. Furthermore, to determine the real-world efficacy of these attacks, we analyze their performance after images undergo degradations associated with social media. Finally, we explore a defense mechanism to bolster resilience against such attacks, an area largely unaddressed in existing literature. Our key findings show that:

- I.** Even the most advanced AI-image detectors, including commercial ones, are vulnerable. Methods such as the Diverse Input Attack [25] can significantly impair their ability to distinguish real from AI-generated images, reducing detection accuracy to worse than chance levels (e.g., ROC AUC dropping to as low as 4.1 on Stable Diffusion 1.4 (SD-1.4) dataset). This vulnerability persists even when the attacker does not have internal knowledge of the detector (e.g., black-box scenario).
- II.** The challenges are compounded in real-world settings where images are frequently altered by processes like social media uploads (involving compression, resizing, etc.). Our findings indicate that many adversarial attacks retain their effectiveness despite these degradations. Moreover, these common image alterations can independently degrade the performance of detectors on images, even if not maliciously changed, making reliable detection even more difficult.
- III.** We tested our adversarial examples against a proprietary detection system, HIVE, and showed that commercial systems are also vulnerable to the attacks used. The results have been confirmed by HIVE, and we support them with our findings to improve their system.
- IV.** Despite these vulnerabilities, it is possible to enhance the robustness of AI-image detectors. We demonstrate that incorporating defense strategies, specifically by adapting robust feature extractors like RobustCLIP [26], can improve a detector’s ability to withstand potent adversarial attacks. For instance, defended models maintained significantly higher ROC AUC scores (e.g., 69.0 and 75.7)

under the Diverse Input attack compared to undefended models (near 0) with a generally modest trade-off in performance on non-attacked (benign) images. Nonetheless, even with robust features, our performance does not match that of a non-malicious scenario, indicating the necessity for alternative approaches to prevent the misuse of GenAI.

2. Background

Recent advancements in image generation and synthetic image detection have led to notable improvements in quality while reducing the potential for misuse. This section provides a summary of recent developments in image generation and offers an overview of diffusion models (DMs). Additionally, we discuss current detection methods and introduce the concept of adversarial examples.

2.1. Image Synthesis

Image synthesis involves learning the underlying probability distribution of a training dataset to generate novel images. This task is particularly challenging in the image domain due to the high dimensionality and diversity of natural images. With deep Boltzmann machines [27] being one of the first generative models, subsequent approaches including variational autoencoders (VAEs) [28], [29], autoregressive models [30]–[32], and generative adversarial networks (GANs) [33]–[36] led to a continuous improvement in image resolution and quality. Notably, multiple studies [4], [37], [38] showed that—for humans—faces generated by models from the StyleGAN family [39]–[41] are practically indistinguishable from real ones.

At the time of writing, DMs [42]–[45] represent the state-of-the-art in image synthesis. DMs feature two processes: During the forward diffusion process, Gaussian noise is gradually added to the image until all original information is lost. The reverse process, which is approximated using a neural network, then learns to iteratively remove some noise to finally obtain a clean image. By initializing the reverse process with random noise, DMs can generate new images from the training data distribution. The key for scaling DMs to higher resolutions is the addition of a pre-trained VAE. Instead of performing the costly forward and backward processes in the high-dimensional image space, latent diffusion models (LDMs) [45] use the lower-dimensional latent space of a pre-trained VAE. Using the VAE’s decoder, the generated latents are then transformed to the high-resolution output image. By introducing cross attention, LDMs can be used for tasks like text-to-image generation, leading to popular tools such as Stable Diffusion [2] or Midjourney [1]. Due to their practical relevance and widespread use, we focus on images generated by LDMs in this work.

2.2. Detection of Synthetic Images

Due to the potentially harmful consequences of photorealistic synthetic images, a variety of detection methods have been proposed. We refer to the recent work of

Tariang et al. [46] for a more detailed overview. In summary, there are three main groups: methods that exploit high-level artifacts, those based on low-level artifacts, and data-driven approaches. Methods in the first group target semantic inconsistencies and, therefore, are usually only applicable to certain subjects or scenes. Examples are impossible eye reflections [47], facial asymmetries [48], or geometric errors [49]. In contrast, methods based on low-level forensic artifacts do not depend on the semantic content of an image. Instead, they rely on invisible traces of the generative process, like frequency artifacts [50]–[52], artificial fingerprints [53], [54], or, specifically for images generated by DMs, properties that can be revealed by “inverting” an image using the forward/backward processes [55].

Finally, the most common approach for detecting generated images is to learn discriminative features from the data itself. Training standard CNNs, like ResNet-50 [56], on real and generated images has been shown to be surprisingly effective [18], [19], [57]. However, developing detectors that can adapt to unseen generative models is an ongoing challenge. Recently, several works [20], [21], [58] have shown that using large vision foundation models (e.g., CLIP [22]) can help towards training such universal detectors. These methods train a relatively simple classifier on top of the features extracted by the pre-trained model, resulting in good generalization capabilities and higher robustness to perturbations. A possible explanation is that by using the pre-trained feature extractor, the detector does not overfit on specific artifacts of a certain generative model, but learns to identify more general properties of synthetic images. In our work, we focus on data-driven approaches due to their generalizability but also because of their inherent vulnerability to adversarial attacks.

2.3. Adversarial Examples

The objective of an adversarial attack against AI-generated image detectors is to generate a perturbed image x_{adv} that remains nearly indistinguishable from the original generated image x yet is classified by the detector as real. The perturbed image x_{adv} is called an adversarial example. The task of finding such adversarial examples can be formulated as a constrained optimization problem:

$$x_{\text{adv}} = \arg \max_{x'} L(f(x'), y) \quad \text{s.t.} \quad \|x' - x\|_p \leq \epsilon,$$

where y represents the ground-truth label, $\|\cdot\|_p$ denotes the ℓ_p -norm, and $L(\cdot)$ is typically the cross-entropy loss. The parameter ϵ defines the maximum allowed distortion between x and x_{adv} . Adversarial attacks can generally be grouped into white-box and black-box methods. Under the white-box scenario, the attacker has complete knowledge of the detector’s parameters and architecture, allowing the use of gradient-based techniques. In contrast, black-box attacks restrict the adversary to querying the target model or using a surrogate model to approximate its gradients.

3. Methodology

In this work, we systematically evaluate the performance of state-of-the-art detection methods under realistic adversarial attack scenarios. To this end, we have curated a diverse collection of datasets that includes images generated by various state-of-the-art generative models alongside a wide range of real images. We further utilize a series of attack methods and degradations to assess the effectiveness of current detection methods.

3.1. Datasets

Our analysis employs three different datasets, namely Synthbuster [59], Chameleon [60], and the newly introduced GPT-4o dataset [61]. These datasets collectively offer a broad spectrum of synthetic and real images, enabling a comprehensive evaluation of detection methods.

Synthbuster. To avoid dataset biases [62] and ensure a fair evaluation of detection methods, we incorporate the Synthbuster dataset [59]. This dataset features 1000 images generated by nine state-of-the-art diffusion models, namely GLIDE [63], Stable Diffusion 1.3 and 1.4 [2], Stable Diffusion XL [64], DALL-E2 [65], DALL-E3 [66], Midjourney [1], and Firefly [67]. Real images are taken from the RAISE-1k dataset [68], which offers 1000 uncompressed photographs spanning diverse categories, thus avoiding artifacts introduced by JPEG compression. The synthetic images are designed to replicate the same objects and scenes present in the real images. Prompts for image generation were obtained using CLIP Interrogator [69] and Midjourney’s `/describe` command, and then manually refined to achieve photorealistic outputs.

Chameleon. The Chameleon dataset [60] offers a challenging benchmark for AI-generated image detection by focusing on images that are indistinguishable from real ones by human standards. Every synthetic image in the dataset has passed a human perception “Turing Test”, demonstrating its deceptive realism. The dataset covers diverse categories such as human, animal, object, and scene, and features high-resolution images (ranging from 720P to 4K), simulating real-world quality. Synthetic images are sourced from user-created content on popular AI art communities, whereas the real images are obtained by applying identical search queries to online photo repositories like Unsplash.

GPT-4o. The GPT-4o dataset consists of images generated by the GPT-4o model (as of April 3rd 2025), based on the evaluation framework presented in GPT-ImgEval [61]. Specifically, these images are the outputs of GPT-4o when prompted with inputs for text-to-image generation, instruction-guided image editing, and world knowledge-informed semantic synthesis. The images were collected using automation scripts that interacted with the GPT-4o web interface. Since there are no real images in the dataset, we reuse the real images from the Synthbuster dataset.

3.2. Detectors

For our evaluation, we consider four state-of-the-art AIGI image detectors that have demonstrated high accuracy and robust generalization in detecting DM-generated images: Corvi [19], UnivFD [20], and DRCT [21] (both Conv-B and CLIP versions). These detectors were chosen to span a diverse range of concepts, architectures, and training paradigms.

Corvi. This detector’s architecture was originally proposed by Gragnaniello et al. [19] and builds upon the influential work of Wang et al. [18]. Both methods leverage a ResNet-50 [56] and rely on heavy data augmentation during training. The notable improvement is the removal of the initial down-sampling layer, which preserves high-frequency information at the cost of a higher number of trainable parameters. Their experiments demonstrate that this design generalizes well across images generated by various GANs, despite being trained exclusively on images generated by ProGAN [36]. Corvi et al. [57] retrained the same architecture on images generated by LDMs [45], demonstrating its capacity to detect DM-generated images.

UnivFD. Ohja et al. [20] address universal fake image detection by leveraging a large vision model, specifically CLIP-ViT-L/14 [70], as a fixed feature extractor. A single linear layer is then trained on top of these pre-extracted features, while the CLIP weights remain frozen. This decoupled training approach, which avoids adapting the feature space to the detection task, improves the detector’s generalization. As a result, UnivFD achieves an average precision of 93.38 across various generative models, including both GANs and DMs.

DRCT. Diffusion reconstruction contrastive training (DRCT) [21] is a training paradigm that enhances existing AIGI image detectors by augmenting the training set with challenging pairs of images. In this framework, pairs of images are generated by processing a real image through both the forward and backward stages of a Stable Diffusion model [45], producing a reconstructed image that closely resembles the original but contains artifacts from the generative process. Together with a contrastive learning objective, this approach trains the detector to distinguish these difficult cases, thereby improving its generalizability to images from unknown generators. Two checkpoints are provided: DRCT-ConvB, which employs a ConvNeXt Base backbone [71], and DRCT-CLIP, which utilizes CLIP-ViT-L/14—the same backbone used by UnivFD.

3.3. Attacks

For our adversarial evaluation, we simulate a realistic black-box threat model where attackers have limited knowledge of the target detector. In this setting, we generate adversarial examples using a range of simple yet effective methods known for their strong transferability. We group these attack methods into two categories: transfer-based attacks and query-based attacks.

Transfer-based attacks. Transfer-based attacks craft adversarial examples using a substitute model that approximates the target detector’s behavior. Since many open-source AIGI detection models are readily available, an attacker can easily select one or more surrogates to optimize the perturbations. One advantage of transfer-based attacks is that adversarial examples can be generated entirely offline, requiring only a single query to the target model for verification. This makes the approach both computationally efficient and stealthy. However, the success of such attacks heavily depends on how well the surrogate approximates the target detector. For this category of attacks, we select four different methods:

- **Projected Gradient Descent (PGD):** PGD [72] is an iterative attack that starts from a random initialization within an allowed range around the original image, and perturbs that image by taking successive steps in the direction that maximizes the loss, while ensuring that the overall perturbation remains imperceptible. Formally, given an input image x , PGD generates adversarial examples x_{adv} by iteratively applying:

$$x_{adv}^{t+1} = \Pi_{\epsilon}(x_{adv}^t - \alpha \cdot \text{sign}(\nabla_x \mathcal{L}(x_{adv}^t, y))) \quad (1)$$

where Π_{ϵ} projects the perturbation onto an ℓ_{∞} -ball of radius ϵ , α is the step size, and \mathcal{L} is the loss function.

- **Ensemble based:** The ensemble-based attack [73] extends PGD to multiple surrogate models $\{f_1, \dots, f_K\}$ with corresponding weights w_k . The gradient update is computed as:

$$\nabla_{ens} = \sum_{k=1}^K w_k \nabla_x \mathcal{L}_k(x_{adv}^t, y) \quad (2)$$

where \mathcal{L}_k is the loss function for model k . The weights are normalized to sum to 1, and the same projection and step size constraints as PGD are applied.

- **Diverse Input Attack:** This method [25] improves transferability by incorporating input diversity into the ensemble attack. At each iteration, it applies random resizing and optional padding:

$$T(x) = \begin{cases} \text{resize}(x, s \cdot H) & \text{with prob. } p_{resize} \\ x & \text{otherwise} \end{cases} \quad (3)$$

where $s \sim U(s_{min}, s_{max})$ is the random scale factor. We use $p_{resize} = 0.8$, $s_{min} = 0.8$, $s_{max} = 1.2$. The gradient is then computed on the transformed input:

$$\nabla_{div} = \sum_{k=1}^K w_k \nabla_x \mathcal{L}_k(T(x_{adv}^t), y) \quad (4)$$

- **Universal perturbations:** This attack aims to find a single perturbation δ that causes misclassification when added to any input image. Given a set of images $\{x_1, \dots, x_N\}$, the perturbation is updated iteratively:

$$\delta^{t+1} = \Pi_{\epsilon}(\delta^t - \alpha \cdot \text{sign}(\frac{1}{N} \sum_{i=1}^N \nabla_x \mathcal{L}(x_i + \delta^t, y_i))) \quad (5)$$

Our implementation maintains two perturbations: one for making fake images appear real and another for making real images appear fake. We utilized this attack in our experiment in the ensemble mode as it is more effective.

Query-based attacks. In contrast to transfer-based methods, query-based attacks exploit direct interaction with the target detector. Instead of utilizing surrogate models, the attacker sends carefully crafted inputs—via an API or other communication channels—to the detector and uses the returned labels or confidence scores to approximate the gradient direction. We examine one representative method:

- **Query-efficient attack:** This approach [74] leverages Natural Evolution Strategies to estimate gradients with limited queries. For each iteration, it samples n Gaussian noise vectors $\{\epsilon_i\}_{i=1}^n$ with scale σ and estimates the gradient as:

$$\hat{\nabla} = \frac{1}{n\sigma} \sum_{i=1}^n \mathcal{L}(x + \sigma\epsilon_i, y)\epsilon_i \quad (6)$$

3.4. Degradations

To complement the adversarial threat model, we also study quality degradations that naturally arise on social media platforms. Xu et al. [75] showed that the degradation induced by real-world social media platforms can be simulated using common transformations. To assess detector performance under both benign and adversarial conditions in real-world scenarios, we adopt the degradation settings introduced by the authors:

- **Medium Degradation:** To simulate social media degradation, images are downsampled to 75% of their original size, and JPEG compression with a quality factor of 50 is applied.
- **High Degradation:** Severe image quality loss is achieved by combining four types of degradation: Gaussian blurring (kernel size 5×5 , $\sigma = 1$, $\mu = 1$), downsampling to 50% of the original size, heavy JPEG compression with a quality factor of 20, and the addition of Gaussian noise ($\mu = 1$, $\sigma = 0.1$).

4. Robustness Analysis

In this section, we present a comprehensive analysis of the adversarial robustness of four state-of-the-art detectors. To establish a baseline, we initially report the detectors’ performance in a benign setting on images from a variety of generative models. We subsequently perform a robustness analysis comprising five attacks in a black-box setting and investigate the effectiveness and quality of the resulting adversarial examples. Then, we test how image degradations, as they commonly occur when images are uploaded to, e.g., a social media platform, impact the effectiveness of the attacks, followed by a case study targeting a closed-source online detection tool. Finally, we showcase that deploying

a simple defense mechanism can significantly enhance the robustness of the detectors against the strongest attack.

4.1. Benign Setting

We first assess the performance of our detectors under benign, non-adversarial conditions. To ensure a fair and comprehensive evaluation, all detectors were trained on the same data and tested on images from a broad range of generative models. These results serve as a baseline for our adversarial robustness analysis.

Setup. For DRCT-CLIP and DRCT-ConvB we use publicly available checkpoints trained on the SD-1.4 train subset from GenImage [76]. Since no matching checkpoints are available for UnivFD and Corvi, we re-train both models on the SD-1.4 subset according to the authors’ instructions. We evaluate our detectors on Synthbuster, Chameleon and most recent GPT-4o images. We report both the area under the receiver-operating characteristic curve (ROC AUC), measuring how well real and generated images can be separated irrespective of a certain threshold, as well as the accuracy given a fixed decision threshold of 0.5.

Results. Table 1 shows the detection performance in the benign setting. Unsurprisingly, the SD-1.4 subset from Synthbuster can be detected very accurately (95.7–100.0 ROC AUC), since the generative models and processing correspond to the training data. The results for SD1.3 are almost equal due to the similarity between both versions of Stable Diffusion. For the particularly challenging Chameleon dataset, which were rated as indistinguishable from real images by human annotators, UnivFD performs best with an ROC AUC of 78.8, but only 57.0 accuracy, suggesting that 0.5 is not the optimal threshold for this dataset. Considering the averaged scores across all datasets, DRCT-CLIP achieves the best performance (92.3 ROC AUC), followed by UnivFD (81.5 ROC AUC), DRCT-ConvB (83.8 ROC AUC), and Corvi (78.1 ROC AUC). In general, we observe that for all detectors, the performance significantly depends on the generative model as well as the processing, demonstrating the limited generalizability of state-of-the-art AI-generated image detectors.

4.2. Clean Attack Setting

We next examine the adversarial robustness of our AI-generated image detectors by testing their performance on adversarial examples created using different attacks. Note that adversarial examples are “clean” in the sense that they are not degraded by common image processing, e.g., resizing or compression.

Setup. We use the L_∞ norm with $\epsilon = 8/255$ for all attacks and a step size of $2/255$ for all transfer-based attacks. We run PGD, ensemble-based, and diverse input attack for ten steps, while the universal perturbation attack requires 50 steps due to the harder optimization problem. For the query-efficient attack we use a maximum of 500

Metric	Detector	Synthbuster					Chameleon	GPT-4o	Avg.				
		SD-1.3	SD-1.4	SD-2	SD-XL	Midjourney 5				Firefly	Glide	DALL-E 2	DALL-E 3
ROC AUC	UnivFD	95.9	95.7	91.9	92.6	92.7	94.0	87.7	79.1	98.8	78.8	99.1	91.5
	DRCT-CLIP	97.1	97.1	96.0	94.9	87.3	94.0	96.7	88.4	98.7	70.0	94.9	92.3
	DRCT-ConvB	98.9	98.5	79.5	88.9	82.5	83.1	86.4	80.5	67.9	67.0	88.5	83.8
	Corvi	100.0	100.0	52.3	73.7	80.0	59.1	77.3	70.9	87.3	65.0	93.7	78.1
	<i>Average</i>	98.0	97.8	79.9	87.5	85.6	82.6	87.0	79.7	88.2	70.2	94.1	86.4
Accuracy	UnivFD	88.7	88.9	80.8	82.5	83.7	85.7	77.4	68.4	93.8	57.0	94.9	82.0
	DRCT-CLIP	90.7	91.0	89.9	87.8	79.0	86.6	90.4	79.0	93.1	45.1	87.3	83.6
	DRCT-ConvB	94.3	94.1	57.5	66.2	59.4	59.5	65.8	59.3	54.7	63.7	67.8	67.5
	Corvi	99.6	99.6	51.2	52.9	51.6	49.5	50.9	50.4	53.3	58.3	60.2	61.6
	<i>Average</i>	93.3	93.4	69.9	72.4	68.4	70.3	71.1	64.3	73.7	56.0	72.5	73.7

TABLE 1: **Baseline Performance.** ROC AUC and accuracy in the benign setting. We test all detectors on the Synthbuster (results for different generators listed separately), Chameleon, and GPT-4o datasets. The rightmost column shows the average performance across all datasets. **Bold** values indicate the best performance per generator.

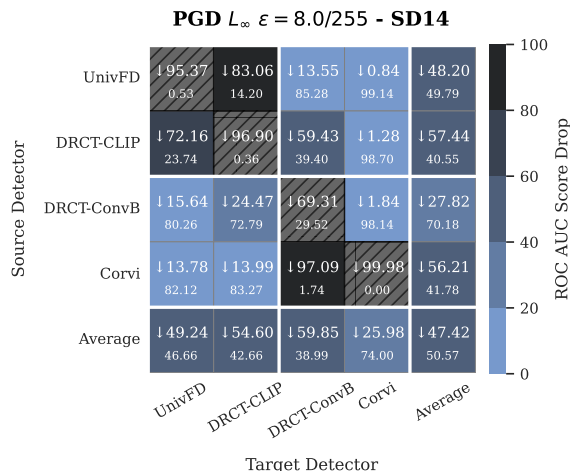


Figure 1: **Transferability Analysis.** Heatmap illustrating the effectiveness of transferring adversarial examples between different detectors. The x-axis represents the source detector used to generate the adversarial examples, while the y-axis represents the target detector. Large numbers show ROC AUC drop; smaller ones below show post-attack ROC AUC.

queries and 50 samples per draw for the gradient estimation alongside a noise scale $\sigma = 0.005$ and a minimum step size of $\epsilon \cdot 0.01$. For each attack configuration, we compute ROC AUC based on adversarial examples created from 1500 images (consisting of 500 from each dataset, 250 fake and 250 real images). In the case of Synthbuster, we limit our analysis to images generated by SD-1.4 due to the detectors’ good performance in the benign setting.

Attack Comparison. Table 2 presents our adversarial robustness analysis in the clean setting, without degradations. Standard **PGD** attacks, when transferred between models, are largely ineffective, though exceptions occur when the source and target models are well aligned (e.g., PGD attacks from DRCT-CLIP significantly impact UnivFD, dropping the ROC AUC from 95.9 to 15.9 on SD-1.4). However,

attacks from a different source, such as DRCT-ConvB, are less effective (ROC AUC drops to 76.8). We analyze PGD transferability in Figure 1, highlighting strong transfers between CLIP-based detectors (UnivFD and DRCT-CLIP) and weaker transfers from CNN-based sources (DRCT-ConvB, Corvi) to CLIP-based targets. While Corvi shows considerable robustness to transferred PGD attacks, white-box analyses (diagonal of Figure 1) confirm that this does not imply inherent immunity when PGD is directly optimized on the target.

To counter the limited transferability of individual PGD, **Ensemble-based Attacks**, specifically a Leave-Target-Out (LTO) ensemble, prove more effective. Adversarial examples crafted against an ensemble of all detectors except the target reduce the average ROC AUC across detectors to 23.4 on SD-1.4 (down from 58.6 for PGD), though Corvi remains resilient (ROC AUC 84.6). The **Diverse Input Attack**, an enhancement of this ensemble approach, is even more successful, reducing the average ROC AUC to a mere 4.1 on SD-1.4 and significantly degrading Corvi’s performance (ROC AUC 14.4).

Alternatively, an attacker might employ a **Universal Perturbation Attack**, seeking a single perturbation applicable to any image class (real/fake). While universal perturbation is less effective than ensemble or diverse image-specific attacks, they still pose a significant threat as they can be added to an image on the fly, without any computation and shared easily. They achieve an average ROC AUC of 46.9 on SD-1.4, outperforming PGD transfer attacks (58.6 ROC AUC) – a trend observed across other datasets like Chameleon (27.4 vs 38.8) and GPT-4o (36.0 vs 49.0). In contrast, a **Query-efficient Attack**, is one of the least effective in our setup. We report an average ROC AUC of 79.7 on SD-1.4. This decrease in attack performance is likely due to the restricted query budget and sampling strategy.

Overall, our findings show that while PGD attacks have limited transferability, ensemble-based attacks significantly improve adversarial effectiveness, especially when combined with input diversity. Universal perturbations offer a modest improvement over standard PGD and are far easier

Attack	Target	Source	SD1.4				Chameleon				GPT-4o				
			Benign	Attacked			Benign	Attacked			Benign	Attacked			
				No Deg.	Med Deg.	High Deg.		No Deg.	Med Deg.	High Deg.		No Deg.	Med Deg.	High Deg.	
PGD	UnivFD	DRCT-CLIP	95.9	15.9	57.2	62.2	79.2	21.8	52.2	63.9	99.2	16.4	75.2	66.0	
		DRCT-ConvB	95.9	76.8	81.9	67.1	79.2	81.4	79.3	68.7	99.2	83.4	94.1	69.1	
		Corvi	95.9	76.2	80.3	71.3	79.2	73.7	72.6	68.8	99.2	82.6	92.5	70.7	
	DRCT-CLIP	UnivFD	97.3	8.7	45.4	60.8	70.7	8.8	43.6	70.4	95.0	5.0	26.5	46.0	
		DRCT-ConvB	97.3	64.6	73.3	62.2	70.7	70.2	77.3	75.8	95.0	52.0	55.0	49.4	
		Corvi	97.3	72.8	78.1	64.9	70.7	67.8	73.9	74.7	95.0	50.3	63.0	50.5	
	DRCT-ConvB	UnivFD	98.8	75.6	61.0	53.2	69.6	33.3	32.5	41.1	88.5	66.6	67.3	46.6	
		DRCT-CLIP	98.8	24.8	50.2	55.2	69.6	5.6	28.2	40.2	88.5	18.8	56.9	45.3	
		Corvi	98.8	1.4	6.9	48.0	69.6	0.0	2.4	40.0	88.5	0.7	7.2	40.5	
	Corvi	UnivFD	100.0	95.5	82.4	57.2	63.0	27.3	25.3	33.2	93.3	67.1	54.3	57.3	
DRCT-CLIP		100.0	94.0	83.9	58.0	63.0	26.2	29.9	37.4	93.3	62.5	59.9	57.3		
DRCT-ConvB		100.0	96.3	86.6	62.6	63.0	49.8	42.3	38.5	93.3	83.0	73.7	59.6		
Average	-	98.0	58.6	65.6	60.2	70.6	38.8	46.6	54.4	94.0	49.0	60.5	54.9		
Ensemble	UnivFD	LTO	95.9	0.0	45.6	64.7	79.2	0.0	43.4	61.8	99.2	0.0	65.6	64.5	
		DRCT-CLIP	97.3	0.9	50.5	62.6	70.7	0.9	54.6	72.0	95.0	0.1	31.5	46.7	
		DRCT-ConvB	98.8	8.1	26.8	50.2	69.6	0.9	6.8	36.4	88.5	6.3	29.5	44.8	
		Corvi	100.0	84.6	76.3	54.1	63.0	19.3	28.2	34.9	93.3	47.0	53.0	54.8	
	Average	-	98.0	23.4	49.8	57.9	70.6	5.3	33.3	51.3	94.0	13.4	44.9	52.7	
Diverse	UnivFD	LTO	95.9	0.0	6.4	51.7	79.2	0.1	3.7	43.9	99.2	0.1	8.0	48.2	
		DRCT-CLIP	97.3	0.6	7.6	52.9	70.7	0.6	9.3	59.6	95.0	0.1	4.0	37.3	
		DRCT-ConvB	98.8	1.5	7.6	43.0	69.6	0.1	2.0	28.3	88.5	2.7	12.8	39.7	
		Corvi	100.0	14.4	23.4	43.7	63.0	0.4	4.8	24.8	93.3	3.1	14.8	49.1	
	Average	-	98.0	4.1	11.3	47.8	70.6	0.3	5.0	39.2	94.0	1.5	9.9	43.6	
Universal	UnivFD	LTO	95.9	20.8	74.0	63.6	79.2	31.5	76.8	69.3	99.2	33.7	87.2	62.9	
		DRCT-CLIP	97.3	56.9	64.8	61.6	70.7	49.9	74.6	74.3	95.0	39.0	57.4	47.6	
		DRCT-ConvB	98.8	23.9	24.4	51.4	69.6	5.8	18.3	38.6	88.5	9.3	26.6	46.4	
		Corvi	100.0	85.8	65.2	53.4	63.0	22.3	34.6	37.6	93.3	62.0	60.5	54.7	
	Average	-	98.0	46.9	57.1	57.5	70.6	27.4	51.1	55.0	94.0	36.0	57.9	52.9	
Query	UnivFD	-	95.9	64.1	74.7	66.9	79.2	60.4	64.2	69.0	99.2	74.1	91.0	70.3	
		DRCT-CLIP	-	97.3	79.0	75.9	64.1	70.7	61.0	72.1	75.7	95.0	72.9	60.5	48.1
		DRCT-ConvB	-	98.8	77.2	63.1	54.8	69.6	33.5	35.2	42.3	88.5	63.4	64.8	47.9
		Corvi	-	100.0	98.5	86.0	51.9	63.0	24.6	31.4	37.2	93.3	70.4	55.0	57.0
	Average	-	98.0	79.7	74.9	59.4	70.6	44.9	50.7	56.1	94.0	70.2	67.8	55.8	

TABLE 2: **Adversarial Robustness.** ROC AUC for different attacks and degradations. We evaluate the “Target” detectors with adversarial examples created using the “Source” detector. “LTO” (leave target out) indicates that the ensemble contains all detectors except for the target. Results in the “Benign” columns correspond approximately to those in Table 1, with slight differences due to sampling variation. The “Attacked” columns contain the scores on adversarial examples with no, medium, and high degradation.

Detector	SD-1.4			Chameleon			GPT-4o			Cross-Dataset Avg.			Overall Avg.
	No Deg.	Medium Deg.	High Deg.	No Deg.	Medium Deg.	High Deg.	No Deg.	Medium Deg.	High Deg.	No Deg.	Medium Deg.	High Deg.	
UnivFD	95.9	90.2	88.1	79.2	80.4	84.6	99.2	98.0	96.5	91.4	89.5	89.7	90.2
DRCT-CLIP	97.3	80.2	77.2	70.7	70.4	81.1	95.0	68.9	63.0	87.7	73.2	73.8	78.2
DRCT-ConvB	98.8	92.1	40.3	69.6	67.0	45.4	88.5	82.0	54.6	85.6	80.4	46.8	70.9
Corvi	100.0	99.9	77.5	63.0	56.8	38.0	93.3	75.3	52.3	85.4	77.4	55.9	72.9

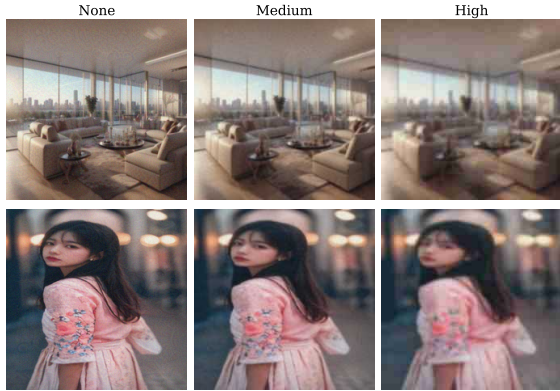
TABLE 3: **Degradation Performance Analysis.** ROC AUC comparison on clean and degraded inputs. “No Deg.” denotes unmodified images, while “Medium” and “High” indicate increasing levels of degradation. No attack has been performed in this setting.

to deploy, making them a practical threat. In contrast, query-efficient attacks remain the least effective in our evaluation and appear less promising under current constraints.

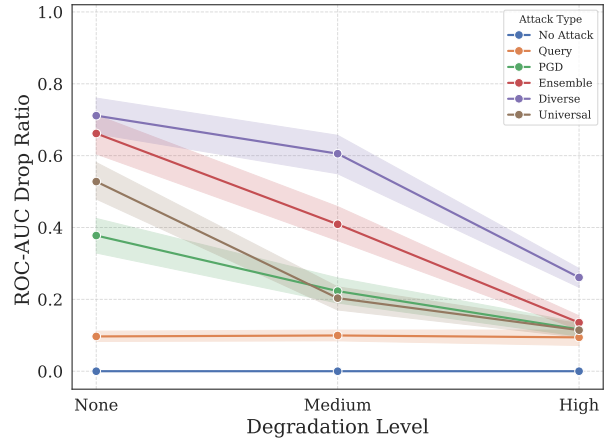
4.3. Attacks in Real-world Scenarios

While the previous analysis demonstrates attack effectiveness in a clean setting, real-world scenarios introduce additional complexities. Therefore, we consider attacks in a real-world setting, where adversarial examples, spread via social media or messaging apps, frequently undergo transformations such as resizing and compression, as shown

by Xu et al. [75]. Our analysis assumes an attacker aims to evade detection across various degradation levels (none, medium, high) encountered in an image’s digital lifecycle, rather than focusing on less common, specific edits. To have a fair comparison and measure the attack effectiveness without any bias, we first report the benign detector performance over these degradations in Table 3 (with sample degradations illustrated in Figure 2a) demonstrates that while most detectors are generally robust to these transformations on benign images, their performance is slightly affected. CLIP-based detectors (UnivFD and DRCT-CLIP) exhibit greater robustness, potentially due to their reliance on high-level features.



(a)



(b)

Figure 2: **Analysis of Degradation Effects.** (a) Visual comparison showing how different degradation methods affect adversarial examples. (b) Quantitative analysis of degradation impact on attack’s performance.

In contrast, CNN-based detectors (DRCT-ConvB and Corvi), which depend more on low-level features, are consequently more affected by these (often low-level) transformations, even though such common transformations are part of the training set for all detectors. Notably, for the Chameleon dataset, UnivFD and DRCT-CLIP can surprisingly improve with degradation, likely as the applied transformations make very high-resolution images more similar to their training data. This performance on benign, degraded images serves as the baseline.

To assess whether adversarial attacks remain effective under real-world transformations, we apply the previously discussed attacks to images that are then subjected to these degradations. The overall impact on detector performance is detailed in Table 2 and further illustrated in Figure 2b. Notably, Figure 2b quantifies the reduction in adversarial effectiveness using the ROC AUC drop ratio (calculated as ROC AUC drop divided by the clean ROC AUC). This metric is useful because it normalizes for the detector’s baseline performance, allowing for fairer comparison across attacks.

In general, most attacks become less effective after transformation, although they can still pose a substantial threat. The **Diverse Input attack** shows greater robustness to degradation compared to the **Ensemble attack**, as evidenced by a smaller performance drop from the “None” to “Medium” degradation levels. We hypothesize that this is due to the incorporation of resizing into the adversarial example generation process, which helps the attack generalize better under transformation. In contrast, the **Universal attack** is the least robust, suffering a significant performance decline from no degradation to medium degradation. This is expected, as universal perturbations are generic and intended to work across an entire dataset; even minor alterations can render them ineffective.

In conclusion, while the ROC AUC drop ratio indicates that transformations reduce the effectiveness of adversarial

attacks, even the strongest degradation levels do not completely neutralize adversarial noise.

4.4. Adversarial Example Quality Analysis

We also analyze the quality of adversarial examples, as it is crucial to ensure they are not only effective in evading detection but also maintain high visual fidelity.

Setup. Qualitative examples of adversarial examples for different attacks can be found in Figure 3. For the quantitative evaluation, we employ five widely-used metrics: Mean Perturbation, Peak Signal-to-Noise Ratio (PSNR), Structural Similarity Index (SSIM), Learned Perceptual Image Patch Similarity (LPIPS) [77], and Deep Image Structure and Texture Similarity (DISTS) [78] selected to capture different aspects of image quality, including perceptual similarity and structural integrity. These metrics are computed between adversarial examples and their original counterparts in the clean setting, as constant degradation applied to both would not alter their relative quality. For a unified and holistic measure, we compute a normalized average of these five metrics with similar weights, presented as “Quality” (0-100, with 100 being the highest similarity) in Table 4.

Quality-Attack Success Trade-off. The results in Table 4 reveal a strong correlation between an attack’s success (ROC AUC drop ratio) and the visual quality of the generated adversarial examples. For instance, the Ensemble attack and Universal attack demonstrate quality on par with the PGD attack, yet their ROC AUC drop ratios are substantially higher (0.95 for Ensemble and 0.76 for Universal, compared to 0.54 for PGD), indicating greater effectiveness while preserving similar visual fidelity. Conversely, the Diverse Input attack, which yields the highest ROC AUC drop ratio (0.98), exhibits the lowest quality. To facilitate a fair comparison, we plot the ROC AUC drop ratio against the Normalized Quality Score for three distinct ϵ ($4/255$, $8/255$,

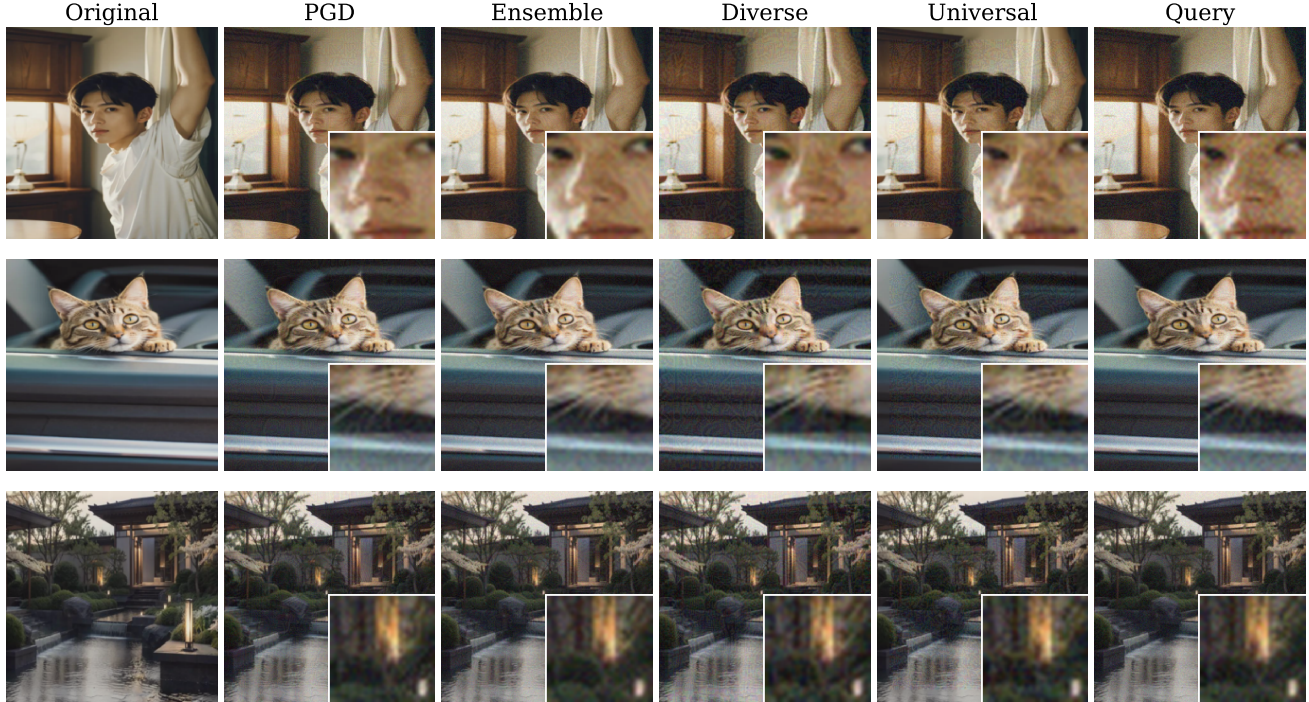


Figure 3: Adversarial Examples generated for target UnivFD with $\epsilon = 8/255$. Images are from the Chameleon dataset.

Attack	Image Quality Metrics					Performance		
	Mean Pert. \downarrow	SSIM \uparrow	PSNR \uparrow	LPIPS \downarrow	DISTS \downarrow	Quality \uparrow	ROC Drop Ratio \uparrow	
PGD	0.077	0.917	33.97	0.093	0.127	58.12	0.542	
Ensemble	0.076	0.921	34.07	0.092	0.122	59.27	0.950	
Diverse	0.108	0.871	31.63	0.161	0.165	40.73	0.980	
Universal	0.020	0.875	32.48	0.156	0.140	55.14	0.764	
Query	0.058	0.943	49.52	0.053	0.079	81.82	0.114	

TABLE 4: **Attack Quality Analysis.** Comparison of different attack methods across image quality metrics and performance indicators. Lower (\downarrow) is better for perturbation and perceptual metrics, while higher (\uparrow) is better for SSIM, PSNR, Quality, and ROC Drop.

and 16/255) in Figure 4. This analysis shows a significant quality decrease with increasing ϵ , while the corresponding increase in ROC AUC drop ratio is not as pronounced for attacks like PGD, Ensemble, Diverse Input, and Query-efficient. This demonstrates that an attacker, by carefully selecting the attack method and an appropriate ϵ , can achieve a high ROC AUC drop ratio while maintaining a high level of visual fidelity.

4.5. Case Study

Our analysis identifies the Diverse Input attack as highly effective, achieving a significant ROC AUC drop ratio while producing good quality images with an appropriate epsilon value. To assess its real-world applicability, we conducted a case study on HIVE [79], a widely-used closed-source online AIGI detector. Using HIVE’s free web interface, we tested the Diverse Input attack (with an ensemble of all four of our detectors as sources) on 20% of images from

Metric	Dataset	Attacked		
		Benign	$\epsilon = 4/255$	$\epsilon = 8/255$
ROC AUC	SD1.4	100.0	90.3	73.8
	Chameleon	98.2	83.4	79.7
	Average	99.0	87.0	76.6
Accuracy (Real/Fake)	SD1.4	100.0 / 100.0	66.0 / 90.0	56.0 / 76.0
	Chameleon	98.0 / 92.0	56.0 / 86.0	48.0 / 92.0
	Average	99.0 / 96.0	61.0 / 88.0	52.0 / 84.0

TABLE 5: **Case Study.** Performance under adversarial attacks showing ROC AUC and Real/Fake Accuracy (%) under different perturbation bounds

the Synthbuster and Chameleon datasets from our initial experiments; this sample size was constrained by HIVE’s interface limits. Table 5 presents the results. Notably, in the benign setting, commercial detectors like HIVE significantly outperform their academic counterparts, with HIVE

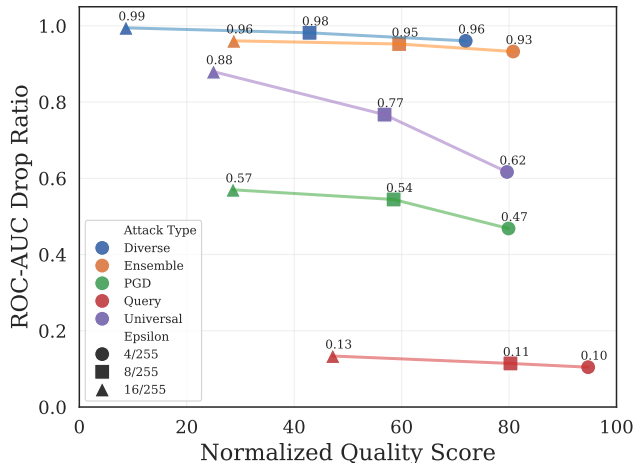


Figure 4: **ROC AUC Drop Ratio vs. Quality.** Comparison of three ϵ for tested attacks. Image quality decreases notably with larger ϵ (lower quality score), while ROC AUC remains relatively stable, suggesting that small ϵ values suffice for effective attacks with high image quality.

achieving near-perfect ROC AUC scores on both datasets. However, when attacked with $\epsilon = 8/255$, HIVE’s ROC AUC dropped from 99.0 to 73.8 on Synthbuster and from 98.2 to 79.7 on Chameleon. Another key observation is the asymmetric impact of adversarial perturbation on real versus fake images. At $\epsilon = 8/255$, HIVE’s accuracy on real images dropped by 47% (from 99% to 52%), while for fake images it declined by only 12% (from 96% to 84%). This suggests that adversarial perturbations tend to introduce artifacts that mimic characteristics of synthetic images, making it easier to misclassify real images as fake than the reverse.

We reached out to HIVE and shared our findings, which they have since validated. We are now collaborating with them to employ these insights in improving their system.

4.6. Towards Defending AIGI Detectors

At a foundational level, AIGI classifiers, like any other machine learning classifier, are vulnerable to adversarial perturbations. However, a critical distinction amplifies the robustness challenge for AIGI detection. Standard classifiers, such as those employed for object recognition, learn to distinguish between categories based on meaningful, semantic differences inherent to the visual data (e.g., the features defining a “cat” versus a “dog”). In contrast, AIGI detectors often rely on identifying subtle, low-level artifacts or statistical fingerprints introduced by the specific generative model used to create an image. As these generative models advance, they become increasingly adept at estimating the true distribution of natural images. This improvement inherently means that the very artifacts AIGI detectors are trained to recognize become less pronounced, or even absent, in the outputs of newer, more sophisticated models. Therefore, the task of robustly detecting AI-generated content becomes

arguably more challenging, as the detectable features upon which AIGI detectors depend diminish over time.

In this context, we explore the potential of adapting existing defense mechanisms. It is important to emphasize that our objective here is not to present this as the definitive or optimal defense. Rather, our aim is to provide a preliminary showcase: to investigate whether established defense paradigms can offer a degree of robustness in this rapidly evolving landscape and to stimulate further research into tailored AIGI defense strategies. Specifically, this section investigates the transfer of a defense strategy from the vision-language model (VLM) literature to the AIGI detection domain.

Robust Feature Extractors. Given that CLIP-based detectors have been shown to provide strong detection and generalization results (refer to Table 1), we adapt an existing defense initially proposed for Vision-Language Models [26] to AIGI detection. Our approach is inspired by Hua et al. [80], who demonstrated the importance of using robust pre-trained models as feature extractors to transfer robustness to downstream tasks. The principle is straightforward: if the feature representation is robust to adversarial perturbations, a linear classifier trained on these features is less likely to change its decision. Hence, we propose to replace the standard CLIP-ViT-L/14 backbone with that of a robust version of CLIP [26]. This robust version, RobustCLIP, ensures that the learned feature representations are perturbation-invariant through unsupervised adversarial fine-tuning. During this fine-tuning, RobustCLIP enhances the robustness of the CLIP vision encoder by ensuring the embeddings of adversarially perturbed images (generated using PGD- L_∞) are close to those of the original images, achieved by minimizing a loss function such as the squared Euclidean distance between these embeddings, while preserving performance on clean data. We use two versions of the robust fine-tuned backbones provided by the authors, corresponding to ϵ values of 2/255 and 4/255, and name our defended models UnivFD-R2 and UnivFD-R4, respectively. We train the linear head on the same data as the original UnivFD model, but with the robust CLIP backbone. The training process remains unchanged, and we use the same hyperparameters as in the original UnivFD model.

Evaluating the Defended Models. The defended models are evaluated against the same attacks and degradations used in previous experiments, focusing on the strongest attack, Diverse Input attack, with $\epsilon = 8/255$. Detailed results are shown in Table 6, with additional results including other attacks and degradations in Table 7 in the Appendix. Table 6 reports ROC AUC scores averaged across all datasets. The defended models demonstrate an improved robustness against the Diverse Input attack: the ROC AUC score of the undefended model drops to nearly 0, while the defended models achieve 69.0 (UnivFD-R2) and 75.7 (UnivFD-R4). This enhanced robustness comes with a slight decrease in benign ROC AUC, from 91.4 for the undefended UnivFD to 88.4 (R2) and 84.4 (R4). Similar improvements are observed for attacks combined with various levels of degradation,

Model	Benign	Attacked		
		No Deg.	Med Deg.	High Deg.
UnivFD	91.4	0.0	6.7	55.7
UnivFD-R2	88.4	69.0	78.8	73.8
UnivFD-R4	84.4	75.7	78.3	74.6

TABLE 6: **Defense Performance against Diverse Attack.** ROC AUC scores for different defense models against the diverse attack with $\epsilon = 8/255$. We evaluate three variants of the UnivFD detector on both benign and adversarial examples with different levels of degradation.

however we do not nearly reach the same performance as in the benign case. The defended models achieve ROC AUC scores of 78.8 (R2) and 78.3 (R4), compared to 6.7 for the undefended UnivFD. Although UnivFD-R4 demonstrates a higher degree of robustness, detector deployers must consider the detector’s susceptibility to attacks and the inherent trade-off between robustness and clean performance.

5. Related Work

Carlini & Farid [23] conducted a pioneering case study on adversarial attacks against forensic classifiers. They showed that detection systems without proper defense can fail in white-box and black-box settings. They covered five different attacks on GAN images on two detectors. Gandhi & Jain [81] explored adversarial attacks on deep-fake detectors proposing Lipschitz regularization and deep image prior (DIP) as defenses. Li et al. [82] introduced a method for generating adversarial anti-forensic images by optimizing within the face manifold in StyleGAN. Their approach showed superior transferability and quality of adversarial images but is limited to StyleGAN generator. Hou et al. [83] designed adversarial statistical consistency attacks to minimize statistical differences between fake and real images. This approach involved adversarially modifying image attributes like exposure and noise. They achieve high transferability across various detectors, but their method is still limited to GAN generated images. Liu et al. [84] proposed a detector-agnostic trace removal attack that looks into the original image generation pipeline and attempts to remove artifacts introduced in the generation process. Huang et al. [85] suggest a retouch method to reduce the artifact in the generated images by performing implicit notch filtering. More recently, Abdullah et al. [24] propose a semantic attack that utilizes a foundation model to craft adversarial samples with semantic manipulation of the image content. Meng et al. [86] propose a new attribute variation-based adversarial attack that perturbs the latent space via a combination of Gaussian prior and semantic discriminator to bypass detection.

Most of the work above has focused on producing new attacks that transfer better or result in higher quality images; however, we demonstrated that even the simple available attacks can achieve these objectives. Additionally, most of the papers discussed here do not focus on diffusion model-

generated images and the detectors that can detect DM images, which represent the current state of the art in image generation. Nearly all the works have suggested defenses without assessing their effectiveness.

6. Discussion

Lack of Definition for AIGI. Detecting AI-generated images is inherently ill-posed due to a lack of consensus on what constitutes AI-generated content. The distinction between entirely AI-created images, those with AI inpainting or editing, and human-edited AI images (e.g., Photoshop) is ambiguous and varies across research domains. This unclear ground truth complicates detection, as different researchers and systems might operate under varying assumptions.

Detection vs. Generation Arms Race. Preventing misuse of AIGI is an arms race between AI generation techniques and detection mechanisms. As soon as a new detection method is developed, generative techniques are devised to circumvent these detectors, propagating a continuous cycle of advancements on both sides. This dynamic nature makes developing persistent solutions for AI-generated content detection challenging.

Context-dependent Detection. AI-generated content is becoming an integral part of everyday life, with its usage expected to rise significantly. As a result, auditing every AI-generated image may become impractical. Instead, the focus should shift toward detecting harmful AI-generated content to identify and mitigate associated risks. For instance, in social media, AI-generated images are more likely to be used in disinformation and scams.

Robustness-Accuracy Trade-off. Enhancing forensic classifier robustness often reduces accuracy on clean data. Deploying these systems requires weighing this trade-off based on the likelihood of attacks. Balancing robustness and accuracy demands careful, context-aware evaluation. In some cases, utility may outweigh full AI-content detection (e.g., less interactive platforms), while others require catching every instance (e.g., news sites). Thus, classification needs must be accurately assessed to align performance with specific use cases.

7. Conclusion

In this study, we show that despite efforts to improve adversarial robustness in forensic classifiers, state-of-the-art AIGI detectors remain vulnerable to attacks. Our findings indicate that adversarial examples transfer across different detectors, posing a significant threat to forensic detection mechanisms. Moreover, real-world degradations, such as those induced by social media post-processing, make detection tasks even more challenging, regardless of the presence of an attacker. This degradation undermines the reliability of forensic systems in real-world scenarios.

Our results on using robust features show that we can improve the robustness of detectors, but do not reach an

equal performance as in benign settings. We argue that to prevent the misuse of GenAI, we need clear definitions, better risk assessments, and alternative solutions that take into account the context of misuse.

Acknowledgments

This work was supported by the German Federal Ministry of Education and Research under the grants AIGenCY (16KIS2012) and SisWiss (16KIS2330). It was also funded by the Deutsche Forschungsgemeinschaft (DFG, German Research Foundation) under Germany's Excellence Strategy – EXC 2092 CASA – 390781972. Partial funding was provided by the VolkswagenStiftung through the Niedersächsisches Vorab program (ZN3695). SM was partially supported by the Saarbrücken Graduate School of Computer Science.

References

- [1] Midjourney, “Midjourney,” <https://www.midjourney.com/home>, 2024, accessed: 2024-01-01.
- [2] Stability AI, “Stable Diffusion,” <https://stability.ai/stable-image>.
- [3] Black Forest Labs, “FLUX,” <https://blackforestlabs.ai/#get-flux>.
- [4] J. Frank, F. Herbert, J. Ricker, L. Schönherr, T. Eisenhofer, A. Fischer, M. Dürmuth, and T. Holz, “A representative study on human detection of artificially generated media across countries,” in *IEEE Symposium on Security and Privacy (SP)*, 2024.
- [5] Europol Innovation Lab, “Facing reality? law enforcement and the challenge of deepfakes,” <https://www.europol.europa.eu/publications-events/publications/facing-reality-law-enforcement-and-challenge-of-deepfakes>, 2024.
- [6] Federal Bureau of Investigation (FBI), Cyber Division, “Malicious actors almost certainly will leverage synthetic content for cyber and foreign influence operations,” <https://www.ic3.gov/Media/News/2021/210310-2.pdf>, 2021.
- [7] J. Ricker, D. Assenmacher, T. Holz, A. Fischer, and E. Quiring, “AI-generated faces in the real world: A large-scale case study of Twitter profile images,” in *International Symposium on Research in Attacks, Intrusions and Defenses (RAID)*, 2024.
- [8] M. Spring, “Trump supporters target black voters with faked ai images,” Mar 2024. [Online]. Available: <https://www.bbc.com/news/world-us-canada-68440150>
- [9] B. McCarthy, “Image of Biden planning military action in fatigues is fake,” Apr 2024. [Online]. Available: <https://factcheck.afp.com/doc.afp.com.34H74GF>
- [10] N. Robins-Early, “How did Donald Trump end up posting Taylor Swift deepfakes?” *The Guardian*, 2024, <https://www.theguardian.com/technology/article/2024/aug/24/trump-taylor-swift-deepfakes-ai>.
- [11] The White House, “Executive order on the safe, secure, and trustworthy development and use of artificial intelligence,” 2023, <https://www.whitehouse.gov/briefing-room/presidential-actions/2023/10/30/executive-order-on-the-safe-secure-and-trustworthy-development-and-use-of-artificial-intelligence/>.
- [12] The European Parliament, “Regulation (EU) 2024/1689 of the European Parliament and of the Council,” 2024, <https://eur-lex.europa.eu/eli/reg/2024/1689/oj>.
- [13] P. Fernandez, G. Couairon, H. Jégou, M. Douze, and T. Furon, “The stable signature: Rooting watermarks in latent diffusion models,” in *IEEE/CVF International Conference on Computer Vision (CVPR)*, 2023.
- [14] J. Fei, Z. Xia, B. Tondi, and M. Barni, “Supervised gan watermarking for intellectual property protection,” in *IEEE International Workshop on Information Forensics and Security (WIFS)*, 2022.
- [15] Coalition for Content Provenance and Authenticity (C2PA), “C2PA technical specification,” 2024, https://c2pa.org/specifications/specifications/2.0/specs/C2PA_Specification.html.
- [16] Z. Jiang, J. Zhang, and N. Z. Gong, “Evading watermark based detection of ai-generated content,” in *ACM SIGSAC Conference on Computer and Communications Security (CCS)*, 2023.
- [17] Y. Hu, Z. Jiang, M. Guo, and N. Z. Gong, “A transfer attack to image watermarks,” in *The Thirteenth International Conference on Learning Representations*, 2025. [Online]. Available: <https://openreview.net/forum?id=UchRjcf4z7>
- [18] S.-Y. Wang, O. Wang, R. Zhang, A. Owens, and A. A. Efros, “Cnn-generated images are surprisingly easy to spot... for now,” in *IEEE/CVF conference on computer vision and pattern recognition*, 2020.
- [19] D. Gragnaniello, D. Cozzolino, F. Marra, G. Poggi, and L. Verdoliva, “Are gan generated images easy to detect? a critical analysis of the state-of-the-art,” in *IEEE international conference on multimedia and expo (ICME)*. IEEE, 2021.
- [20] U. Ojha, Y. Li, and Y. J. Lee, “Towards universal fake image detectors that generalize across generative models,” in *IEEE/CVF Conference on Computer Vision and Pattern Recognition*, 2023.
- [21] B. Chen, J. Zeng, J. Yang, and R. Yang, “Drct: Diffusion reconstruction contrastive training towards universal detection of diffusion generated images,” in *International Conference on Machine Learning (ICML)*, 2024.
- [22] A. Radford, J. W. Kim, C. Hallacy, A. Ramesh, G. Goh, S. Agarwal, G. Sastry, A. Askell, P. Mishkin, J. Clark, G. Krueger, and I. Sutskever, “Learning transferable visual models from natural language supervision,” in *Proceedings of the 38th International Conference on Machine Learning*, ser. Proceedings of Machine Learning Research, M. Meila and T. Zhang, Eds., vol. 139. PMLR, 18–24 Jul 2021, pp. 8748–8763. [Online]. Available: <https://proceedings.mlr.press/v139/radford21a.html>
- [23] N. Carlini and H. Farid, “Evading deepfake-image detectors with white- and black-box attacks,” in *2020 IEEE/CVF Conference on Computer Vision and Pattern Recognition Workshops (CVPRW)*, 2020, pp. 2804–2813.
- [24] S. M. Abdullah, A. Cheruvu, S. Kanchi, T. Chung, P. Gao, M. Jadliwala, and B. Viswanath, “An analysis of recent advances in deepfake image detection in an evolving threat landscape,” in *IEEE Security and Privacy (S&P)*, 2024.
- [25] C. Xie, Z. Zhang, Y. Zhou, S. Bai, J. Wang, Z. Ren, and A. L. Yuille, “Improving transferability of adversarial examples with input diversity,” in *2019 IEEE/CVF Conference on Computer Vision and Pattern Recognition (CVPR)*, 2019, pp. 2725–2734.
- [26] C. Schlarmann, N. D. Singh, F. Croce, and M. Hein, “Robust clip: Unsupervised adversarial fine-tuning of vision embeddings for robust large vision-language models,” *ICML*, 2024.
- [27] R. Salakhutdinov and G. E. Hinton, “Deep boltzmann machines,” in *International Conference on Artificial Intelligence and Statistics (AISTATS)*, 2009.
- [28] D. P. Kingma and M. Welling, “Auto-encoding variational bayes,” in *International Conference on Learning Representations (ICLR)*, 2014.
- [29] D. J. Rezende, S. Mohamed, and D. Wierstra, “Stochastic backpropagation and approximate inference in deep generative models,” in *International Conference on Machine Learning (ICML)*, 2014.
- [30] A. van den Oord, N. Kalchbrenner, L. Espeholt, K. Kavukcuoglu, O. Vinyals, and A. Graves, “Conditional image generation with PixelCNN decoders,” in *Advances in Neural Information Processing Systems (NeurIPS)*, 2016.

- [31] A. van den Oord, N. Kalchbrenner, and K. Kavukcuoglu, "Pixel recurrent neural networks," in *International Conference on Machine Learning (ICML)*, 2016.
- [32] T. Salimans, A. Karpathy, X. Chen, and D. P. Kingma, "Pixelcnn++: Improving the pixelcnn with discretized logistic mixture likelihood and other modifications," in *International Conference on Learning Representations (ICLR)*, 2017.
- [33] I. Goodfellow, J. Pouget-Abadie, M. Mirza, B. Xu, D. Warde-Farley, S. Ozair, A. Courville, and Y. Bengio, "Generative adversarial nets," in *Advances in Neural Information Processing Systems (NeurIPS)*, 2014.
- [34] J.-Y. Zhu, T. Park, P. Isola, and A. A. Efros, "Unpaired image-to-image translation using cycle-consistent adversarial networks," in *IEEE International Conference on Computer Vision (ICCV)*, 2017, 2017.
- [35] A. Brock, J. Donahue, and K. Simonyan, "Large scale GAN training for high fidelity natural image synthesis," in *International Conference on Learning Representations (ICLR)*, 2019.
- [36] T. Karras, T. Aila, S. Laine, and J. Lehtinen, "Progressive growing of GANs for improved quality, stability, and variation," in *International Conference on Learning Representations (ICLR)*, 2018.
- [37] B. Shen, B. RichardWebster, A. O'Toole, K. Bowyer, and W. J. Scheirer, "A study of the human perception of synthetic faces," in *IEEE International Conference on Automatic Face and Gesture Recognition (FG)*, 2021.
- [38] S. J. Nightingale and H. Farid, "AI-synthesized faces are indistinguishable from real faces and more trustworthy," *Proceedings of the National Academy of Sciences*, 2022.
- [39] T. Karras, S. Laine, and T. Aila, "A style-based generator architecture for generative adversarial networks," in *Proceedings of the IEEE/CVF Conference on Computer Vision and Pattern Recognition (CVPR)*, 2019.
- [40] T. Karras, S. Laine, M. Aittala, J. Hellsten, J. Lehtinen, and T. Aila, "Analyzing and improving the image quality of StyleGAN," in *Proceedings of the IEEE/CVF Conference on Computer Vision and Pattern Recognition (CVPR)*, 2020.
- [41] T. Karras, M. Aittala, S. Laine, E. Härkönen, J. Hellsten, J. Lehtinen, and T. Aila, "Alias-Free Generative Adversarial Networks," in *Advances in Neural Information Processing Systems (NeurIPS)*, 2021.
- [42] J. Sohl-Dickstein, E. Weiss, N. Maheswaranathan, and S. Ganguli, "Deep unsupervised learning using nonequilibrium thermodynamics," in *International Conference on Machine Learning (ICML)*, 2015.
- [43] J. Ho, A. Jain, and P. Abbeel, "Denoising diffusion probabilistic models," in *Advances in Neural Information Processing Systems (NeurIPS)*, 2020.
- [44] P. Dhariwal and A. Nichol, "Diffusion models beat GANs on image synthesis," in *Advances in Neural Information Processing Systems (NeurIPS)*, 2021.
- [45] R. Rombach, A. Blattmann, D. Lorenz, P. Esser, and B. Ommer, "High-resolution image synthesis with latent diffusion models," in *Proceedings of the IEEE/CVF Conference on Computer Vision and Pattern Recognition (CVPR)*, 2022.
- [46] D. Tariang, R. Corvi, D. Cozzolino, G. Poggi, K. Nagano, and L. Verdoliva, "Synthetic image verification in the era of generative artificial intelligence: What works and what isn't there yet," *IEEE Security and Privacy*, vol. 22, no. 3, p. 37–49, May 2024. [Online]. Available: <https://doi.org/10.1109/MSEC.2024.3376637>
- [47] S. Hu, Y. Li, and S. Lyu, "Exposing GAN-Generated faces using inconsistent corneal specular highlights," in *IEEE International Conference on Acoustics, Speech and Signal Processing (ICASSP)*, 2021.
- [48] F. Matern, C. Riess, and M. Stamminger, "Exploiting visual artifacts to expose deepfakes and face manipulations," in *IEEE Winter Applications of Computer Vision Workshops (WACVW)*, 2019.
- [49] A. Sarkar, H. Mai, A. Mahapatra, S. Lazebnik, D. Forsyth, and A. Bhattad, "Shadows don't lie and lines can't bend! generative models don't know projective geometry...for now," in *Proceedings of the IEEE/CVF Conference on Computer Vision and Pattern Recognition (CVPR)*, 2024.
- [50] X. Zhang, S. Karaman, and S.-F. Chang, "Detecting and simulating artifacts in GAN fake images," in *IEEE International Workshop on Information Forensics and Security (WIFS)*, 2019.
- [51] J. Frank, T. Eisenhofer, L. Schönherr, A. Fischer, D. Kolossa, and T. Holz, "Leveraging frequency analysis for deep fake image recognition," in *International Conference on Machine Learning (ICML)*, 2020.
- [52] J. Ricker, S. Damm, T. Holz, and A. Fischer, "Towards the detection of diffusion model deepfakes," in *International Conference on Computer Vision Theory and Applications (VISAPP)*, 2024.
- [53] F. Marra, D. Gragnaniello, L. Verdoliva, and G. Poggi, "Do GANs leave artificial fingerprints?" in *IEEE Conference on Multimedia Information Processing and Retrieval (MIPR)*, 2019.
- [54] N. Yu, L. S. Davis, and M. Fritz, "Attributing fake images to GANs: Learning and analyzing GAN fingerprints," in *IEEE/CVF International Conference on Computer Vision (ICCV)*, 2019.
- [55] J. Ricker, D. Lukovnikov, and A. Fischer, "Aeroblade: Training-free detection of latent diffusion images using autoencoder reconstruction error," in *IEEE/CVF Conference on Computer Vision and Pattern Recognition (CVPR)*, 2024.
- [56] K. He, X. Zhang, S. Ren, and J. Sun, "Deep residual learning for image recognition," in *2016 IEEE Conference on Computer Vision and Pattern Recognition (CVPR)*, 2016, pp. 770–778.
- [57] R. Corvi, D. Cozzolino, G. Zingarini, G. Poggi, K. Nagano, and L. Verdoliva, "On the detection of synthetic images generated by diffusion models," in *IEEE International Conference on Acoustics, Speech and Signal Processing (ICASSP)*, 2023.
- [58] D. Cozzolino, G. Poggi, R. Corvi, M. Nießner, and L. Verdoliva, "Raising the bar of ai-generated image detection with clip," in *Proceedings of the IEEE/CVF Conference on Computer Vision and Pattern Recognition (CVPR) Workshops*, 2024.
- [59] Q. Bammey, "Synthbuster: Towards detection of diffusion model generated images," *IEEE Open Journal of Signal Processing*, p. 1–9, 2023.
- [60] S. Yan, O. Li, J. Cai, Y. Hao, X. Jiang, Y. Hu, and W. Xie, "A sanity check for AI-generated image detection," in *The Thirteenth International Conference on Learning Representations*, 2025. [Online]. Available: <https://openreview.net/forum?id=ODRHZrkOQM>
- [61] Z. Yan, J. Ye, W. Li, Z. Huang, S. Yuan, X. He, K. Lin, J. He, C. He, and L. Yuan, "Gpt-imgeval: A comprehensive benchmark for diagnosing gpt4o in image generation," 2025. [Online]. Available: <https://arxiv.org/abs/2504.02782>
- [62] D. Arp, E. Quiring, F. Pendlebury, A. Warnecke, F. Pierazzi, C. Wressnegger, L. Cavallaro, and K. Rieck, "Dos and don'ts of machine learning in computer security," in *USENIX Security Symposium*, 2022.
- [63] A. Q. Nichol, P. Dhariwal, A. Ramesh, P. Shyam, P. Mishkin, B. McGrew, I. Sutskever, and M. Chen, "GLIDE: Towards photorealistic image generation and editing with text-guided diffusion models," in *Proceedings of the 39th International Conference on Machine Learning*, ser. Proceedings of Machine Learning Research, K. Chaudhuri, S. Jegelka, L. Song, C. Szepesvari, G. Niu, and S. Sabato, Eds., vol. 162. PMLR, 17–23 Jul 2022, pp. 16 784–16 804. [Online]. Available: <https://proceedings.mlr.press/v162/nichol22a.html>
- [64] D. Podell, Z. English, K. Lacey, A. Blattmann, T. Dockhorn, J. Müller, J. Penna, and R. Rombach, "SDXL: Improving latent diffusion models for high-resolution image synthesis," in *The Twelfth International Conference on Learning Representations*, 2024. [Online]. Available: <https://openreview.net/forum?id=di52zR8xgf>

- [65] A. Ramesh, P. Dhariwal, A. Nichol, C. Chu, and M. Chen, "Hierarchical text-conditional image generation with clip latents," 2022. [Online]. Available: <https://arxiv.org/abs/2204.06125>
- [66] A. Ramesh, P. Dhariwal, C. Chu, I. Mulayoff, J. Yang, A. Sadek, M. Pavlov, F. Hohman, V. Misra, J. Stokes, J. Clark, F. Saucedo, Z. Wang, Y. Zhang, S. Ebrahimi, J. Hilton, R. Jha, J. Walz, B. Dolhansky, A. Madaan, N. Agrawal, P. Katarkar, P. Patil, D. Karpushonak, O. Porat, R. Solay, D. Budden, H. Hu, Y. Lu, L. Angledal, L. Weidinger, J. Teyssedre, S. Steenkiste, L. Ochseneither, S. G. Colmenarejo, M. Malave, M. Clark, E. Sun, J. Ferreira, D. Rubino, V. Chen, A. Go, G. Brockman, D. Ziegler, L. Ouyang, I. Babuschkin, M. Knight, J. Tworek, Y. Bai, D. Amodei, I. Sutskever, J. Leike, P. Christiano, and S. Altman, "Dall-e 3: Art made simple," *OpenAI Research*, 2024. [Online]. Available: <https://cdn.openai.com/papers/dall-e-3.pdf>
- [67] Adobe, "Free generative ai for creatives," <https://www.adobe.com/products/firefly.html>, 2024, accessed: 2024-01-01.
- [68] D.-T. Dang-Nguyen, C. Pasquini, V. Conotter, and G. Boato, "Raise: a raw images dataset for digital image forensics," in *Proceedings of the 6th ACM Multimedia Systems Conference*, ser. MMSys '15. New York, NY, USA: Association for Computing Machinery, 2015, p. 219–224. [Online]. Available: <https://doi.org/10.1145/2713168.2713194>
- [69] "CLIP Interrogator," <https://github.com/pharmapsychotic/clip-interrogator>.
- [70] A. Dosovitskiy, L. Beyer, A. Kolesnikov, D. Weissenborn, X. Zhai, T. Unterthiner, M. Dehghani, M. Minderer, G. Heigold, S. Gelly, J. Uszkoreit, and N. Houlsby, "An image is worth 16x16 words: Transformers for image recognition at scale," in *International Conference on Learning Representations (ICLR)*, 2020.
- [71] Z. Liu, H. Mao, C. Wu, C. Feichtenhofer, T. Darrell, and S. Xie, "A convnet for the 2020s," *2022 IEEE/CVF Conference on Computer Vision and Pattern Recognition (CVPR)*, pp. 11 966–11 976, 2022. [Online]. Available: <https://api.semanticscholar.org/CorpusID:245837420>
- [72] A. Madry, A. Makelov, L. Schmidt, D. Tsipras, and A. Vladu, "Towards deep learning models resistant to adversarial attacks," in *International Conference on Learning Representations*, 2018. [Online]. Available: <https://openreview.net/forum?id=rJzIBfZAb>
- [73] F. Tramèr, A. Kurakin, N. Papernot, I. Goodfellow, D. Boneh, and P. McDaniel, "Ensemble adversarial training: Attacks and defenses," in *International Conference on Learning Representations*, 2018. [Online]. Available: <https://openreview.net/forum?id=rkZvSe-RZ>
- [74] A. Ilyas, L. Engstrom, A. Athalye, and J. Lin, "Black-box adversarial attacks with limited queries and information," in *Proceedings of the 35th International Conference on Machine Learning*, ser. Proceedings of Machine Learning Research, J. Dy and A. Krause, Eds., vol. 80. PMLR, 10–15 Jul 2018, pp. 2137–2146. [Online]. Available: <https://proceedings.mlr.press/v80/ilyas18a.html>
- [75] H. Xu, Y. Wang, Z. Wang, Z. Ba, W. Liu, L. Jin, H. Weng, T. Wei, and K. Ren, "ProFake: Detecting deepfakes in the wild against quality degradation with progressive quality-adaptive learning," in *Proceedings of the 2024 on ACM SIGSAC Conference on Computer and Communications Security*, 2024, <https://dl.acm.org/doi/10.1145/3658644.3690238>.
- [76] Y. Chen, X. Huang, Q. Zhang, W. Li, M. Zhu, Q. Yan, S. Li, H. Chen, H. Hu, J. Yang, W. Liu, and J. Hu, "Gim: A million-scale benchmark for generative image manipulation detection and localization," *Proceedings of the AAAI Conference on Artificial Intelligence*, vol. 39, no. 2, pp. 2311–2319, Apr. 2025. [Online]. Available: <https://ojs.aaai.org/index.php/AAAI/article/view/32231>
- [77] R. Zhang, P. Isola, A. A. Efros, E. Shechtman, and O. Wang, "The unreasonable effectiveness of deep features as a perceptual metric," in *2018 IEEE/CVF Conference on Computer Vision and Pattern Recognition*, 2018, pp. 586–595.
- [78] K. Ding, K. Ma, S. Wang, and E. P. Simoncelli, "Image quality assessment: Unifying structure and texture similarity," *IEEE Transactions on Pattern Analysis and Machine Intelligence*, vol. 44, no. 5, pp. 2567–2581, 2022.
- [79] Hive, "Hive moderation," 2025, accessed: 2025-05-28. [Online]. Available: <https://hivemoderation.com/>
- [80] A. Hua, J. Gu, Z. Xue, N. Carlini, E. Wong, and Y. Qin, "Initialization matters for adversarial transfer learning," in *Proceedings of the IEEE/CVF Conference on Computer Vision and Pattern Recognition*, 2024, pp. 24 831–24 840.
- [81] A. Gandhi and S. Jain, "Adversarial perturbations fool deepfake detectors," in *2020 International Joint Conference on Neural Networks (IJCNN)*, 2020, pp. 1–8.
- [82] D. Li, W. Wang, H. Fan, and J. Dong, "Exploring adversarial fake images on face manifold," in *2021 IEEE/CVF Conference on Computer Vision and Pattern Recognition (CVPR)*, 2021, pp. 5785–5794.
- [83] Y. Hou, Q. Guo, Y. Huang, X. Xie, L. Ma, and J. Zhao, "Evading deepfake detectors via adversarial statistical consistency," in *2023 IEEE/CVF Conference on Computer Vision and Pattern Recognition (CVPR)*, 2023, pp. 12 271–12 280.
- [84] C. Liu, H. Chen, T. Zhu, J. Zhang, and W. Zhou, "Making deepfakes more spurious: Evading deep face forgery detection via trace removal attack," *IEEE Transactions on Dependable and Secure Computing*, vol. 20, no. 6, p. 5182–5196, Nov. 2023. [Online]. Available: <http://dx.doi.org/10.1109/TDSC.2023.3241604>
- [85] Y. Huang, F. Juefei-Xu, Q. Guo, Y. Liu, and G. Pu, "Dodging deepfake detection via implicit spatial-domain notch filtering," *IEEE Transactions on Circuits and Systems for Video Technology*, vol. 34, no. 8, pp. 6949–6962, 2024.
- [86] X. Meng, L. Wang, S. Guo, L. Ju, and Q. Zhao, "Ava: Inconspicuous attribute variation-based adversarial attack bypassing deepfake detection," in *2024 IEEE Symposium on Security and Privacy (SP)*, 2024, pp. 74–90.

Appendix

Attack	Model	SD1.4				Chameleon				GPT-4o			
		Benign	Attacked			Benign	Attacked			Benign	Attacked		
			No Deg.	Med Deg.	High Deg.		No Deg.	Med Deg.	High Deg.		No Deg.	Med Deg.	High Deg.
PGD	UnivFD	95.9	62.0	79.6	68.3	79.2	59.5	72.4	69.2	99.2	68.4	90.7	69.6
	UnivFD-R2	92.5	82.8	83.9	75.8	73.7	69.8	69.7	70.3	98.8	94.4	94.4	80.9
	UnivFD-R4	88.9	82.2	82.5	75.6	66.5	63.6	64.5	65.3	97.7	93.7	92.7	84.8
Ensemble	UnivFD	95.9	0.0	53.8	66.3	79.2	0.1	41.0	63.6	99.2	0.0	66.5	68.1
	UnivFD-R2	92.5	78.8	83.1	75.5	73.7	64.7	68.0	70.1	98.8	92.3	93.9	80.4
	UnivFD-R4	88.9	81.1	82.1	75.4	66.5	62.1	64.0	65.3	97.7	93.1	92.4	84.6
Diverse	UnivFD	95.9	0.0	6.8	57.5	79.2	0.0	3.3	51.3	99.2	0.0	9.9	58.2
	UnivFD-R2	92.5	67.8	80.9	74.4	73.7	54.0	63.0	68.4	98.8	85.0	92.4	78.7
	UnivFD-R4	88.9	77.8	81.2	75.1	66.5	58.3	62.0	64.6	97.7	91.1	91.7	84.2
Universal	UnivFD	95.9	18.5	78.5	67.8	79.2	25.4	75.3	68.8	99.2	17.9	92.7	69.1
	UnivFD-R2	92.5	81.4	84.0	75.7	73.7	70.7	70.1	70.5	98.8	93.4	94.0	80.3
	UnivFD-R4	88.9	82.0	82.5	75.6	66.5	64.2	64.9	65.3	97.7	93.4	92.6	84.7
Query	UnivFD	95.9	84.9	85.5	68.6	79.2	71.8	75.3	69.7	99.2	92.0	94.0	71.1
	UnivFD-R2	92.5	85.1	84.1	76.0	73.7	72.2	70.7	71.2	98.8	95.3	94.5	80.8
	UnivFD-R4	88.9	83.2	82.6	75.5	66.5	65.0	65.3	66.0	97.7	94.1	92.8	84.8

TABLE 7: **Defense Performance.** ROC AUC for different defense models against attacks with $\epsilon = 8/255$. We evaluate three variants of the UnivFD detector: the base model (UnivFD), and two robust versions (UnivFD-R2 and UnivFD-R4). “Benign” columns show performance on non-adversarial examples, while “Attacked” columns contain scores on adversarial examples with no, medium, and high degradation.